34th Annual International Conference of the IEEE EMBS
San Diego, California USA, 28 August - 1 September, 2012

ZPEG: a hybrid DPCM-DCT based approach for compression of Z-stack images

Sourabh Khire[1], Lee Cooper[2], Yuna Park[2], Alexis Carter[3], Nikil Jayant[1], and Joel Saltz[2,3]

Abstract— **Modern imaging technology permits obtaining images at varying depths along the thickness, or the Z-axis of the sample being imaged. A stack of multiple such images is called a Z-stack image. The focus capability offered by Z-stack images is critical for many digital pathology applications. A single Z-stack image may result in several hundred gigabytes of data, and needs to be compressed for archival and distribution purposes. Currently, the existing methods for compression of Z-stack images such as JPEG and JPEG 2000 compress each focal plane independently, and do not take advantage of the Z-signal redundancy. It is possible to achieve additional compression efficiency over the existing methods, by exploiting the high Z-signal correlation during image compression. In this paper, we propose a novel algorithm for compression of Z-stack images, which we term as ZPEG. ZPEG extends the popular discrete-cosine transform (DCT) based image encoder to compress Z-stack images. This is achieved by decorrelating the neighboring layers of the Z-stack image using differential pulse-code modulation (DPCM). PSNR measurements, as well as subjective evaluations by experts indicate that ZPEG can encode Z-stack images at a higher quality as compared to JPEG, JPEG 2000 and JP3D at compression ratios below 50:1.**

I. INTRODUCTION

Whole slide imaging involves the digitization of a glass slide using CCD technology, thus enabling users to view high-resolution digital images of tissue sections, smears and other samples on an electronic display. Once digitized, these images can be easily and interactively shared over the Internet [1]. Further, whole slide images (WSIs) remove the reliance on physical space and equipment for storing and viewing conventional glass slides, and in contrast to glass slides, are not susceptible to damage and fading over time. Due to these advantages, WSIs are widely used in teaching, and in some cases have replaced conventional light microscopy [2].

Most WSIs consist of a single focal plane. However, images acquired at a single focal depth are not sufficient for assessment of structures such as thick smears, folded tissue sections and other three-dimensional (3D) cell groups. Acquiring images at various focal planes is also helpful for identifying cells undergoing division (mitotic figures), which is a critical measurement in evaluating many cancers. To replicate the focus capability of the optical microscope in the digital domain, it is necessary to construct 3D slides composed of multiple WSIs acquired along the thickness, or Z-axis, of the sample [3], [4]. This collection of multiple images is called a Z-stack image. Z-stack images can find applications in cytology and morphology studies, brain-mapping and analysis of any samples demonstrating variations along the Z-axis. However, uncompressed Z-stack images result in extremely large files. For example, a 20mm x 15mm region digitized with a resolution of 0.25 microns/pixel, using an objective lens with 40x magnification and an eyepiece with 10x magnification results in an image containing 80000x60000 or 4.8 giga-pixels. When represented with 24 bits per pixel (bpp), this image results in a file size of around 15 gigabytes (GB). Since a Z-stack image is composed of multiple WSIs, the size of the entire Z-stack image can be in the order of several hundred gigabytes. For a hospital, which may scan hundreds of Z-stack images in a single day, archiving these uncompressed images is nearly impossible. Further, transmission of such large images results in unacceptably long latencies. Clearly, some form of image compression is required to squeeze these huge images down to more manageable sizes.

Although Z-stack imaging is a relatively recent innovation in the domain of digital pathology, 3D medical imagery in the form of X-ray radiography, computed tomography (CT) and magnetic resonance imaging (MRI) has long existed in the field of radiology. Further, multispectral and hyperspectral images have been commonly used in remote sensing, geology and mining. To compress these volumetric images, techniques employing 3D transforms such as 3D DCT [5] and 3D wavelets [6] have been proposed in literature. Further, JPEG 2000 Part-2 (multi-component transform (MCT)) and the JPEG 2000 3D (Part 10 or JP3D) have been used for compression of radiology images [7], [8]. Similarly, a combination of 3D DCT and hybrid DPCM-DCT, as well as JP3D has been employed for compression of hyperspectral imagery [9], [10]. To the best of our knowledge, the application of 3D image compression algorithms in digital pathology has not been investigated so far. Currently, all commercially available slide scanners compress the scanned Z-stack images using the JPEG [11] or the JPEG 2000 [12] compression standards [13]. These standards were originally designed to compress two-dimensional (2D) images. To compress Z-stack images using 2D image compression algorithms, each focal plane of the Z-stack is treated as an independent image. However, this method does not take into account the inherent Z-signal correlation of the Z-stack image, and results in a significant loss of compression efficiency. To exploit the redundancy along the Z-direction, we propose a novel compression algorithm which we term as ZPEG. ZPEG extends the popular

[1]School of Electrical and Computer Engineering, Georgia Institute of Technology, Atlanta, GA 30332, USA.

[2] Center for Comprehensive Informatics, Emory University, Atlanta, GA 30322, USA.

[3]Department of Pathology and Laboratory Medicine, Emory University School of Medicine, Atlanta, GA 30322, USA.

DCT-based image encoder such as JPEG, to compress a stack of correlated images. This is achieved by employing transform-domain DPCM to decorrelate neighboring layers of the Z-stack. In the following sections, we will describe the proposed scheme in detail.

II. Compression of Z-stack Images

Z-stack images are formed by acquiring multiple WSIs at different depths along the thickness of the sample. A key result of acquiring images in this manner is the introduction of a strong Z-signal redundancy within the Z-stack image. Fig. 1 shows different focal planes (or layers) of a single Z-stack image. As seen from this sequence of images, cell-groups appear to sharpen or fade progressively across various layers along the Z-axis. Fig. 2(b) shows the correlation coefficient (ρ) between the planes of the Z-stack image shown in Fig. 2(a). As seen from Fig. 2(b), even for a lag of six layers, the autocorrelation coefficient along the Z-axis is very high ($\rho \approx 0.99$), indicating a very strong Z-signal correlation. For all the Z-stack images in our database, we found that the autocorrelation coefficient never drops below 0.95 across the entire stack, indicating that all the layers of the Z-stack image are fairly correlated. 2D image-compression algorithms such as JPEG and JPEG 2000 employ a 2D transform to spatially decorrelate the image, but fail to exploit this strong Z-signal redundancy, thus resulting in a loss of compression efficiency. ZPEG overcomes this limitation of 2D image encoders by using DPCM to exploit the interlayer redundancy within Z-stack images.

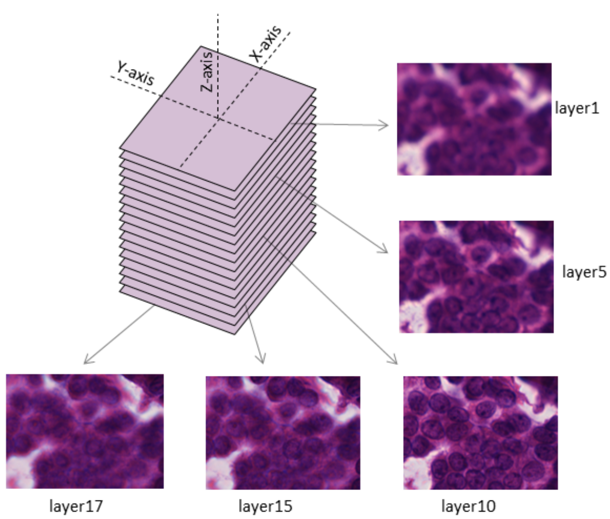

Fig. 1. Different layers of a single Z-stack image.

The term ZPEG is inspired from the popular JPEG standard, and was chosen because ZPEG essentially extends JPEG to three dimensions. Fig. 3 shows a block diagram of a transform-based 2D image encoder. The main blocks of such encoders are the forward transform, the quantizer and the entropy encoder. Forward transforms such as the DCT or the Discrete Wavelet Transform (DWT) exploit the spatial redundancy within the image by spatially decorrelating the neighboring pixels of the image. The quantizer irreversibly

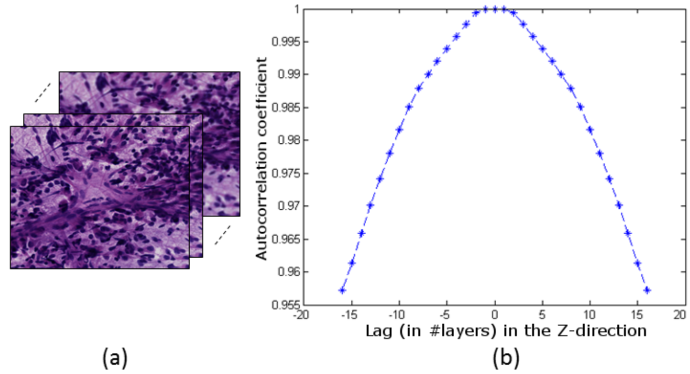

Fig. 2. Z-signal correlation within a Z-stack image.

quantizes these transformed coefficients, and the entropy encoder losslessly compresses these quantized coefficients to generate the compressed bitstream. In JPEG, the forward transform of choice is the 2D DCT. The DCT coefficients are quantized using standard or custom quantization tables and losslessy compressed using a combination of run-length and Huffman encoding to generate the JPEG bitstream. The JPEG decoder shown in Fig. 3 performs the inverse of all the operations carried out by the encoder. Thus the decoder "unpacks" the encoded bit-stream to generate the quantized DCT coefficients. This is followed by inverse quantization and a 2D inverse DCT (IDCT) to reconstruct the individual pixels of the image.

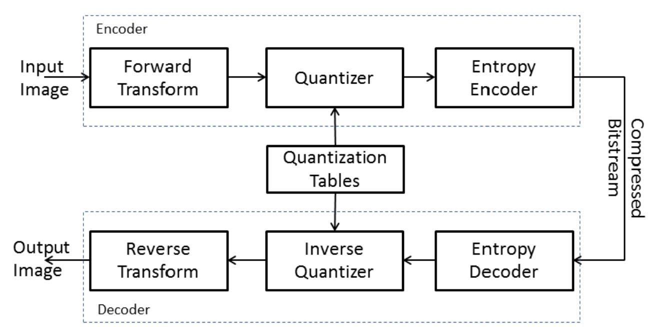

Fig. 3. Block diagram of a transform-based image encoder and decoder.

To extend a 2D image encoder to the three dimensions, we employ a hybrid DPCM-DCT based approach. Fig. 4 shows the block diagram of a simple DPCM codec [14]. In a DPCM-based encoder, neighboring pixels are decorrelated by generating an "estimate" or a predicted pixel, and then computing a "residual" by subtracting the predicted pixel from the input pixel. This residual is further quantized, encoded and transmitted. In its simplest form, the predicted pixel can be generated using a linear predictor. The decoder reverses the operations performed by the DPCM encoder to reconstruct the output pixel.

Fig. 5 shows the block diagram of the proposed ZPEG algorithm. The encoding starts by spatially decorrelating neighboring pixels of each layer using the 2D DCT. Next, the DPCM encoder exploits the Z-signal correlation by

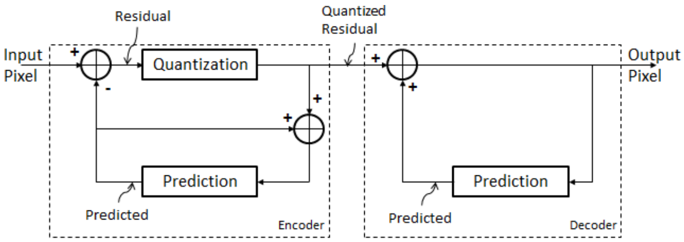

Fig. 4. Block diagram of a DPCM-based image encoder and decoder.

generating a "predicted layer" corresponding to each input layer. For computation simplicity, and to avoid the overhead of signaling the predictor coefficients to the decoder, the predicted layer in our scheme is simply the previous encoded layer. Thus the residual generated by the DPCM encoder is essentially a difference image between the current layer and the previously encoded layer. Finally, a JPEG-like entropy encoder losslessly compresses the residual to generate the ZPEG bitstream. The gain in compression efficiency of ZPEG over JPEG is due to the fact that the "energy" of the residual frame is much lower than that of the original frame. Lower energy implies that ZPEG can represent the same information using lesser number of bits as compared to JPEG.

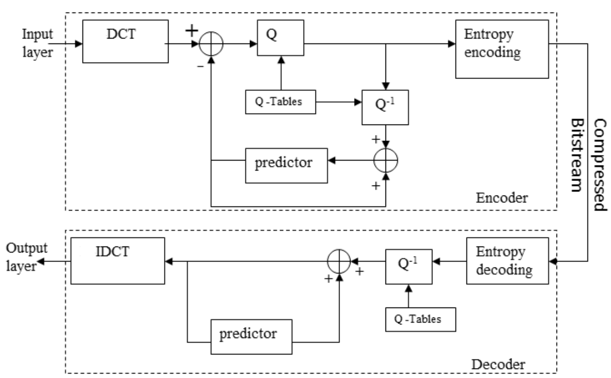

Fig. 5. Block diagram of the ZPEG encoder and decoder.

III. Results and Discussions

Currently, JPEG and JPEG 2000 are the state of the art for compression of Z-stack images. Further, since JP3D has been specifically developed to compress 3D medical imagery [8], [10], we compare the performance of ZPEG against these three image-coding standards. To test the performance of our scheme, we acquired several Z-stack images, and also downloaded some images available online [15]. We imaged several smears using the Hamamatsu Nanozoomer [16] slide-scanner at a magnification of 40x. Each acquired Z-stack image consisted of 17 layers, and each layer had a spatial resolution of approximately 20000x18000 pixels. These Z-stack images were further decomposed into multiple tiles of the size 4096x4096 pixels. These tiles were then encoded using the different image encoders mentioned above. JPEG, JPEG 2000 and JP3D compression was performed using libraries provided by the Independent JPEG group [17] and OpenJPEG [18]. The ZPEG encoder was implemented by us in Matlab. Fig. 6 shows the PSNR for three Z-stack images. As seen in the figure, ZPEG outperforms JPEG in terms of PSNR at all compression ratios. ZPEG also achieves a gain of 0.5 to 1.5 dB over JPEG 2000 and JP3D at compression ratios below 50:1. However, at higher compression ratios JPEG 2000 and JP3D start to outperform ZPEG. It is also interesting to note, that the performance of JPEG 2000 and JP3D remains very similar across all compression ratios.

While PSNR is a simple metric to evaluate compression performance, it does not relate well with the visual quality of the image. Moreover, due to the medical nature of these images they need to be compressed at diagnostically lossless (DL) quality [19]. A digital-pathology image compressed at DL compression ratio is not necessarily mathematically lossless, but a pathologist should still feel comfortable rendering a diagnosis off a DL-compressed image. To compare the DL quality of various compression schemes, we conducted subjective evaluation tests as described below:

- Three Z-stack images (tiles) were chosen for the test. Each image was compressed using JPEG, ZPEG, JPEG 2000 and JP3D and compressed at five different compression ratios varying from 5:1 to 57:1.
- Images were presented for evaluation in a randomized fashion, and in the form of 15 test-sessions. Four compressed images were displayed in each test-session. All images appearing in the same test-session were compressed at the same compression ratio, but using different compression schemes.
- All images were evaluated by five pathology residents who compared, and indicated their preference towards one or more of the four images displayed in each test-session. The evaluators were blind to the compression scheme and the compression ratio used for each image.

Once all the responses were received, a "winner" was determined for each of the 15 test-sessions. The winner is the compression scheme that received the most number of votes. Table I shows the amount of "wins" accumulated by each scheme. As seen from Table I, ZPEG was not the outright winner, but did receive the most number of wins. This implies that ZPEG was not the preferred choice of compression scheme for every test-session, but was chosen more frequently over the other schemes.

TABLE I
Total number of wins for each compression algorithm.

Image-coding scheme	Number of wins
JPEG	1
JP3D	4
JP2K	6
ZPEG	9

The subjective evaluations also indicate that the performance of the ZPEG algorithm was consistent across all the evaluated compression ratios. For example, ZPEG was a winner for an image compressed at the lowest compression ratio

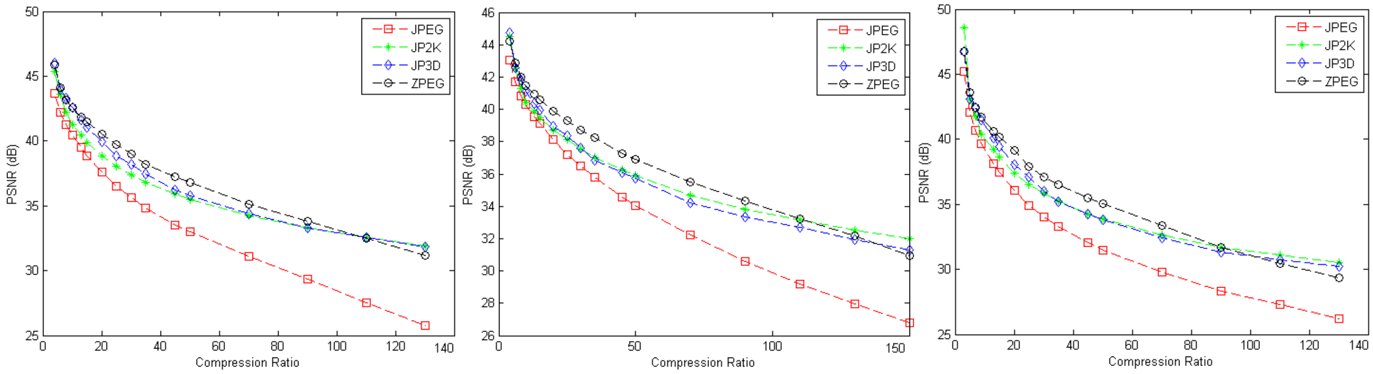

Fig. 6. PSNR vs. compression ratio for some images in the database.

of 5:1 as well as the highest compression ratio of 57:1. All other schemes have a rather inconsistent performance as seen in the Table II. The evaluators were also prompted to provide qualitative comments regarding each image. Some of the comments that we received were, "good brightness/contrast", "best resolution" and "better nuclear detail", justifying the winner in each case.

TABLE II
PERFORMANCE OF DIFFERENT COMPRESSION SCHEMES AT VARIOUS COMPRESSION RATIOS (CR)

CR	Winner	CR	Winner
5:1	JP2K or ZPEG	10:1	JP3D, JP2K or ZPEG
14:1	JP2K	17:1	JP2K or JP3D
25:1	ZPEG	27:1	ZPEG
28:1	JP2K	32:1	JPEG
36:1	JP2K, JP3D or ZPEG	43:1	ZPEG
48:1	ZPEG	55:1	ZPEG
57:1	ZPEG		

IV. CONCLUSIONS

Existing methods for compression of Z-stack images such as JPEG and JPEG 2000 compress each focal plane independently, and do not take advantage of the Z-signal redundancy. In this paper, we proposed a hybrid DPCM-DCT based approach for compression of Z-stack images, which we termed as ZPEG. The ZPEG image compression algorithm exploits the interlayer redundancies existing within the Z-stack image using a hybrid DPCM-DCT based scheme. Objective results indicate that ZPEG finds utility at lower or diagnostically lossless compression ratios, while JPEG 2000 and JP3D lend themselves better for applications involving more aggressive compression. Subjective results indicate that although ZPEG is not universally favored, ZPEG compressed images are more frequently preferred over Z-stack images compressed using JPEG, JPEG 2000 or JP3D.

REFERENCES

[1] M. Lundin *et al.*, "A digital atlas of breast histopathology: an application of web based virtual microscopy," *Journal of Clinical Pathology*, vol. 57, no. 12, pp. 1288–1291, December 2004.

[2] F. J. Weaker and D. C. Herbert, "Transition of a dental histology course from light to virtual microscopy," *Journal of Dental Education*, vol. 73, no. 10, pp. 1213–1221, October 2009.

[3] T. Kalinski *et al.*, "Virtual 3D microscopy using multiplane whole slide images in diagnostic pathology," *American journal of clinical pathology*, vol. 130, no. 2, pp. 259–264, August 2008.

[4] L. Pantanowitz, "Digital images and the future of digital pathology," *Journal of pathology informatics*, vol. 1:15, August 2010.

[5] K. K. Chan *et al.*, "Visualization and volumetric compression," *Proceedings of the SPIE*, vol. 1444, pp. 250, February 9991.

[6] Z. Xiong *et al.*, "Lossy-to-lossless compression of medical volumetric data using three-dimensional integer wavelet transforms," *IEEE Transactions on Medical Imaging*, vol. 22, no. 3, pp. 459 –470, March 2003.

[7] B. Kim *et al.*, "JPEG2000 3D compression vs 2D compression: An assessment of artifact amount and computing time in compressing thin-section abdomen CT images," *Medical Physics*, vol. 36, no. 3, pp. 835–844, March 2009.

[8] T. Kimpe *et al.*, "Compression of medical volumetric datasets: physical and psychovisual performance comparison of the emerging JP3D standard and JPEG2000," *Proceedings of the SPIE*, vol. 6512, pp. 65124L, February 2007.

[9] G. P. Abousleman, M. W. Marcellin, and B. R. Hunt, "Compression of hyperspectral imagery using the 3-D DCT and hybrid DPCM/DCT," *IEEE Transactions on Geoscience and Remote Sensing*, vol. 33, no. 1, pp. 26 –34, January 1995.

[10] J. Zhang *et al.*, "Evaluation of JP3D for lossy and lossless compression of hyperspectral imagery," in *IEEE International Geoscience and Remote Sensing Symposium*, July 2009, vol. 4, pp. IV–474 –IV–477.

[11] G. K. Wallace, "The JPEG still picture compression standard," *IEEE Transactions on Consumer Electronics*, vol. 38, no. 1, pp. xviii –xxxiv, February 1992.

[12] A. Skodras, C. Christopoulos, and T. Ebrahimi, "The JPEG 2000 still image compression standard," *IEEE Signal Processing Magazine*, vol. 18, no. 5, pp. 36 –58, September 2001.

[13] M. G. Rojo *et al.*, "Critical comparison of 31 commercially available digital slide systems in pathology," *International journal of surgical pathology*, vol. 14, no. 4, pp. 285–305, October 2006.

[14] R. C. Gonzalez and R. E. Woods, *Digital Image Processing*, chapter 8.5, pp. 459 – 492, Prentice Hall Inc., Boston, Massachusetts, second edition, 2002.

[15] Aperio, "3D Z-stack images," Available: `http://images2.aperio.com/zstacks/`, [accessed 8-March-2012].

[16] Hamamatsu, "NanoZoomer 2.0-HT slide scanner features and benefits," Available: `http://sales.hamamatsu.com/assets/pdf/hpspdf/e_ndp20.pdf`, [accessed 8-March-2012].

[17] Independent JPEG Group, "The IJG library," Available: `http://www.ijg.org/`, [accessed 8-March-2012].

[18] OpenJPEG, "The OpenJPEG library," Available: `http://www.openjpeg.org/`, [accessed 8-March-2012].

[19] S. M. Williams, A. B. Carter, and N. S. Jayant, "Diagnostically lossless compression of pathology image slides," in *Advancing Practice Instruction and Innovation through Informatics Conference*, October 2008.